SURFACE SCIENCE

Preventing mussel adhesion using lubricant-infused materials

Shahrouz Amini,[1,2]* Stefan Kolle,[3,4]* Luigi Petrone,[1]* Onyemaechi Ahanotu,[3] Steffi Sunny,[4] Clarinda N. Sutanto,[1] Shawn Hoon,[5] Lucas Cohen,[3,4] James C. Weaver,[3] Joanna Aizenberg,[3,4]† Nicolas Vogel,[6]† Ali Miserez[1,7]†

Mussels are opportunistic macrofouling organisms that can attach to most immersed solid surfaces, leading to serious economic and ecological consequences for the maritime and aquaculture industries. We demonstrate that lubricant-infused coatings exhibit very low preferential mussel attachment and ultralow adhesive strengths under both controlled laboratory conditions and in marine field studies. Detailed investigations across multiple length scales—from the molecular-scale characterization of deposited adhesive proteins to nanoscale contact mechanics to macroscale live observations—suggest that lubricant infusion considerably reduces fouling by deceiving the mechanosensing ability of mussels, deterring secretion of adhesive threads, and decreasing the molecular work of adhesion. Our study demonstrates that lubricant infusion represents an effective strategy to mitigate marine biofouling and provides insights into the physical mechanisms underlying adhesion prevention.

Marine biofouling, the process by which marine organisms attach to underwater structures, represents a major economic burden for maritime industries (*1*, *2*). Fouling organisms that settle on submerged surfaces increase hydrodynamic drag, lower ship maneuverability, and, in turn, increase fuel consumption (*3*–*5*). Biofouling also has detrimental consequences on port and fishery infrastructures—for example, by severely clogging circulation piping. Strategies to prevent biofouling are thus a key challenge (*6*–*8*).

Mussels attach indiscriminately to hydrophilic and hydrophobic solid surfaces via adhesive elastomeric protein-based filaments (byssal threads) (*9*, *10*). Attachment plaques at the distal end of byssal threads comprise mussel foot proteins (Mfps) enriched with the posttranslationally modified 3,4-dihydroxy-L-phenylalanine (Dopa) (*11*) that promotes underwater adhesion through various cooperative mechanisms involving removal of hydrated surface salts, as well as delivery of the glue in the form of a complex fluid that does not disperse in aqueous media (*12*–*16*). These specialized proteins enable mussels to adhere to virtually any surface, including metals, minerals, plastics, cements, and even low-surface-energy fluoropolymers (*9*, *12*, *13*).

Lubricant-infused surfaces have recently emerged as a new class of repellent coatings with promising biofouling prevention capacities (*17*–*22*). These surfaces operate by the confinement of a liquid lubricant overlayer, which is immiscible and unreactive with the contaminated medium, onto a solid substrate to protect it from the direct contact with the fouling material (*17*, *23*, *24*). Stable, liquid-protected surfaces can be designed via two general strategies. First, the lubricant can be infused into chemically functionalized roughness features to facilitate spreading and retention through van der Waals and capillary forces (*17*, *24*–*26*). Second, a polymer network can be infused with the lubricant to form a three-dimensional (3D) gel that is bearing a self-replenishing lubricant overlayer (*20*, *27*). Besides the dimensionality (2D versus 3D coating), the two strategies strongly differ in the elastic modulus (E) of the resulting material, with the latter being typically orders of magnitude more compliant. We hypothesized that because lubricant-infused coatings are particularly effective in repelling organic, aqueous, and complex liquids (*17*, *24*, *25*) and reducing fouling by bacteria (*18*–*22*), blood (*28*), and algae (*29*, *30*), they could efficiently prevent mussel adhesion, because the lubricant may shield the underlying solid substrate from being detected by the mussels. Because the adhesion strength of macrofoulers depends on both the material's surface energy γ_s and E (*31*, *32*), we rationalized that the design of the coating (2D roughness versus 3D gel) may affect its antifouling capabilities.

Mussel multichoice assay and settlement

We used the Asian green mussel *Perna viridis* as the model species because it is an abundant marine mussel along the shores of the tropical Indo-Pacific that has invaded other geographical locations through extremely aggressive fouling on boat hulls (*33*). We compared the performance of representative lubricant-infused 3D and 2D materials: (i) 3D polydimethylsiloxane (PDMS) polymer network (~100 μm thick) attached to a glass substrate and infused with silicone oil (*20*), which we term **i**-PDMS, and (ii) 2D silica nanoparticle-based coating deposited by a layer-by-layer technique on glass and infused with the same lubricant (**i**-LBL) (*26*, *28*). As controls, we tested plain glass substrates, the noninfused versions of both materials (labeled PDMS and LBL), as well as two commercially available state-of-the-art foul-release coatings known to reduce marine biofouling on ship hulls, Intersleek700 (IS700) and Intersleek900 (IS900).

A preliminary screening assay (fig. S1) showed that mussel plaques were absent from **i**-PDMS, whereas a small number of plaques was found on **i**-LBL, IS700, and IS900. In contrast, a large number of plaques formed on the three controls (PDMS, LBL, and glass). We then assessed the ability of mussels to dynamically explore substrates and find the most suitable surface on which to attach (Fig. 1A and fig. S2). These multiple-choice assays demonstrated the antifouling performance of **i**-PDMS (only five plaques were deposited in total, all found on a single surface out of 15 immersed **i**-PDMS samples), suggesting that **i**-PDMS fully prevents adhesion and that the fouled sample is likely the result of potential coating defects (Fig. 1, B and C). The commercial standard IS700 exhibited the highest number of plaques per checkerboard (75 ± 10), whereas **i**-LBL and IS900 contained fewer plaques (30 ± 10 plaques per board). Similar 2D coatings with a fluorocarbon surface chemistry/lubricant system exhibited a higher number of adhesive plaques (fig. S3), corroborating previous results on the importance of maximizing the solid/lubricant affinity for the performance of the coating (*28*) [see the supplementary materials (SM), section IIC].

Adhesive strength and secreted adhesive proteins

The adhesion of *P. viridis* is initiated by a time-regulated secretion of foot proteins (Pvfps) forming the final adhesive plaque (*15*). We determined the macroscopic adhesive strength (σ_{ad}) of mussel plaques (Fig. 2A) using a custom-made microtensile testing machine (fig. S4) (*34*, *35*). The mean σ_{ad} was the lowest for infused **i**-PDMS (3.4 ± 2.0 kPa) followed by IS900 (8.1 ± 3.2 kPa), IS700 (20.2 ± 7.4 kPa) and **i**-LBL (20.8 ± 3.6 kPa). The σ_{ad} values for noninfused surfaces were systematically higher (30.3 ± 6.7 kPa for PDMS and 32.4 ± 10.7 kPa for LBL), and the highest adhesive strength was exhibited by bare glass (σ_{ad} = 86.5 ± 23.3 kPa). These data parallel the mussel choice assay findings, with **i**-PDMS outperforming all the other tested surfaces, both in its ability to deter mussel's attachment and to release those few attached plaques with relative ease. Notably, the measured adhesive strength values for the only **i**-PDMS sample with attachment were smaller by a factor of 2 and 5 than those from commercial

[1]Centre for Biomimetic Sensor Science, School of Materials Science and Engineering, Nanyang Technological University (NTU), 50 Nanyang Avenue, Singapore 639798. [2]Energy Research Institute at NTU (ERI@N), Singapore 637553. [3]Wyss Institute for Biologically Inspired Engineering at Harvard University, 60 Oxford Street, Cambridge, MA 02138, USA. [4]John A. Paulson School of Engineering and Applied Sciences, Harvard University, Cambridge, MA 02138, USA. [5]Molecular Engineering Laboratory (MEL), Biomedical Sciences Institutes, Agency for Science, Technology, and Research (A*Star), Singapore. [6]Institute of Particle Technology, Friedrich-Alexander University Erlangen-Nürnberg (FAU), Haberstrasse 9A, 91058 Erlangen, Germany. [7]School of Biological Sciences, 60 Nanyang Drive, NTU, Singapore 637551.
*These authors contributed equally to this work.
†Corresponding author. Email: jaiz@seas.harvard.edu (J.A.); nicolas.vogel@fau.de (N.V.); ali.miserez@ntu.edu.sg (A.M.)

foul-release coatings IS900 and IS700, respectively, and at least one order of magnitude smaller than typical reference surfaces (*34*–*36*).

We complemented the macroscopic adhesion results with biochemical data by analyzing the adsorption of Pvfps in the remnants of adhesive footprints using matrix-assisted laser desorption/ionization–time-of-flight (MALDI-TOF) mass spectrometry (Fig. 2C). This technique is valuable in characterizing the antifouling efficiency at the nanoscale, because there is a direct correlation between the MALDI-TOF signal intensity and the concentration of Pvfps on the surfaces (SM, section IIA) (fig. S5), indicative of increased adsorption. The presence of all adhesive Pvfps was confirmed on the glass substrate controls (Fig. 2C). Although Pvfp-3 gave the higher MALDI-TOF intensity on residual footprints, we consider the detection of Pvfp-5 peaks, even at low intensity (Fig. 2C, insets), to be a more critical signature of adhesion. As the first secreted adhesive protein, Pvfp-5 forms the plaque/substrate molecular interface and plays the key role of priming the surface by displacing surface-bound water before Pvfp-3 and eventually Pvfp-6 are added to form the final adhesive plaque (*15*). All Pvfps were also detected from detached plaque footprints on the noninfused reference surfaces, PDMS, and LBL. In contrast, we did not detect any adhesive proteins on **i**-PDMS after plaque detachment and rinsing. Furthermore, we also verified the absence of purified Pvfp-5 on the infused surfaces after washing (fig. S6). On foul-release coatings IS700, on **i**-LBL, and on other lubricant-infused coatings (fig. S7), a low-intensity peak corresponding to Pvfp-3 was observed, but no Pvfp-5 was detected. No Pvfps were detected on IS900.

Live observation of byssal thread secretion on surfaces

A central question arising from the lack of plaques on **i**-PDMS is whether the surfaces were rejected by the mussels or threads did not stick to the surfaces. We therefore conducted live observations of *P. viridis* feet exploring the surfaces and secreting byssal threads on stiff (LBL) and compliant (PDMS) substrates. On noninfused surfaces, *P. viridis* successfully probed the surface and secreted four and two cured threads on LBL and PDMS, respectively (Fig. 1D; fig. S8, A and B; and movies S1 and S2).

P. viridis probing behavior on infused surfaces was strikingly different. On the **i**-LBL surface, both mussels explored the surface for an appreciable amount of time (30 s and 80 s, respectively) without secreting a thread (fig. S8C and movie S3). This behavior is abnormal, because mussels typically scrub the surface for a few seconds and then spend about 30 s secreting a byssal thread (*37*). On **i**-PDMS, *P. viridis* behaved in three even more unusual ways: (i) the mussel foot explored the surface but did not deposit threads and chose to attach the threads either onto its own shell (Fig. 1E and movie S4) or to reach to a neighboring substrate (movie S5); (ii) the mussel secreted a viscous gel that did not solidify and readily dispersed in seawater (movie S6); and (iii) the mussel extended its foot toward the substrate, but upon scrubbing the surface, swiftly retracted 1 s later without secreting a thread (Fig. 1F and movie S7), suggesting that the mussel either did not detect a solid substrate or refused to commit. A count analysis revealed multiple occurrences of the unusual mussel behaviors (table S1). These observations corroborate the choice assay, where 14 out of 15 **i**-PDMS surfaces were completely plaque-free (Fig. 1, B and C).

Performance of i-PDMS in field studies

To verify that the high antifouling capacity of **i**-PDMS against mussel adhesion in laboratory settings translates into efficient prevention of marine fouling in real-world situations, we conducted field tests in Scituate Harbor (MA, USA) (SM, section IIB) over a period of 16 weeks. We detected only a few newly settled mussels on **i**-PDMS panels, whereas IS900 and PDMS controls showed 4-fold and 30-fold increases in mussel settlements as measured by the total coverage area, respectively (Fig. 3A and table S2). **i**-PDMS outperformed the commercial benchmark and noninfused controls, not only for hard-fouling species, such as mussels, but also for aggressive soft foulers, such as tunicates and hydroids, and microalgal biofilms (slime) (Fig. 3B). These results support the laboratory experiments and show the broad, long-term fouling prevention capacity of **i**-PDMS in complex marine environments.

Analysis of nanoscale contact forces

To reveal what mechanostimulus the mussels may be detecting with their sensing organ, we conducted depth-sensing nanocontact mechanics measurements, which relate to the contact forces experienced by the mussels during probing. Characteristic load-displacement curves (Fig. 4A) showed that contact forces on LBL are expectedly three orders of magnitude larger than on PDMS, with elastic moduli of 83.5 ± 6.8 GPa and 78.8 ± 4.9 GPa for noninfused and infused LBL samples, respectively, and 1.8 ± 0.2 MPa and 0.8 ± 0.1 MPa for PDMS and **i**-PDMS, respectively (fig. S9).

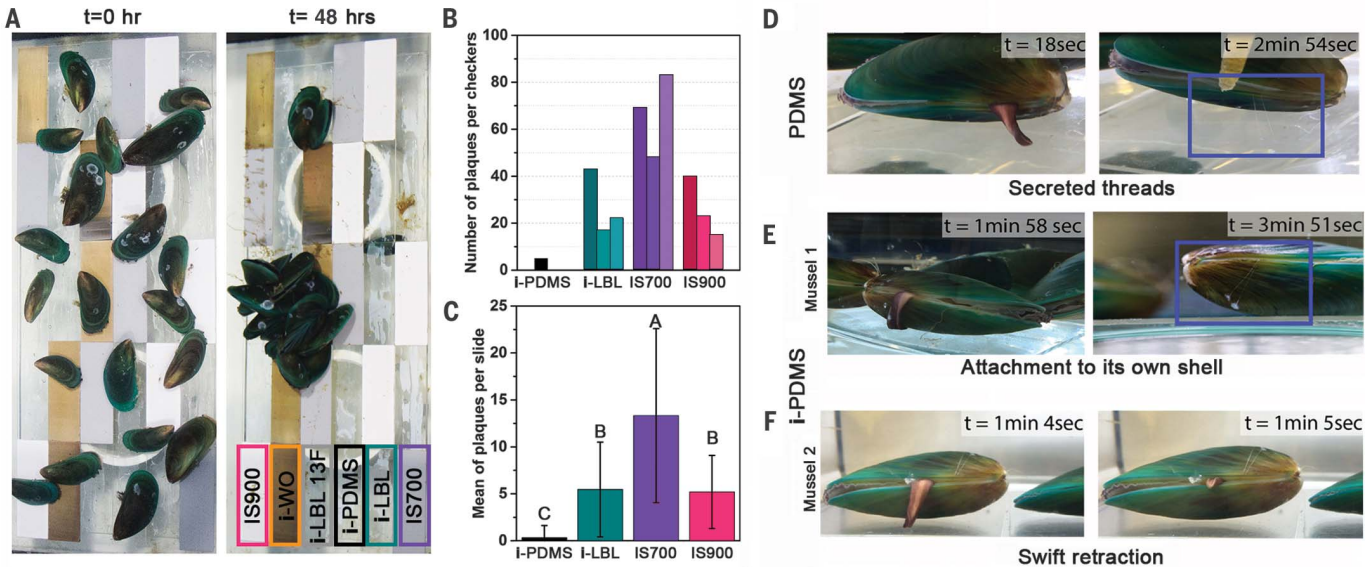

Fig. 1. *P. viridis* mussel settlement and plaque secretion. (**A**) Multiple-choice assay illustrating the randomized checkerboard arrangement of the various surfaces on which mussels were uniformly placed at time zero (left) and allowed to move and settle for 48 hours (right). (**B**) Number of adhesive plaques per surface type in each checkerboard. (**C**) Mean adhesive plaques per slide for each surface type, with bars representing standard error. Significantly different results are labeled with different letters ("A," "B," and "C"). (**D** to **F**) Examples of live observations of *P. viridis* surface exploration and thread secretion on PDMS and **i**-PDMS (see movies S1 to S7). Blue boxes highlight secreted adhesive threads and plaques.

Closer inspection in the low-force region (Fig. 4, B and C) revealed distinct "jump-in" and "jump-off" instabilities detected for both types of infused surfaces. For the **i**-LBL surface (Fig. 4B), a maximum adhesive force in the range 10 to 15 μN was detected upon approach. A similar magnitude of adhesive force value was measured during unloading; however, a much larger displacement was necessary to return to zero force. Because the adhesive forces were absent on the noninfused reference, we attribute them to the formation of a capillary adhesive force when the tip makes contact with the entrapped lubricant (*38*), with a capillary bridge length of 13 μm, as inferred from the retraction portion of loading/unloading cycles. Further focus in the submicrometer displacement range (Fig. 4B, inset) upon approach revealed a nearly constant adhesive force for about 400-nm displacement after the initial jump-in instability, which we attribute to the thickness of the lubricant layer. Subsequently, the force-displacement curves were identical to the reference, indicating direct contact with the solid surface. Therefore, from the "mussel's perspective," **i**-LBL surfaces present a 400-nm-thick lubricant layer after an initial capillary adhesion, during which no solid surface would be sensed.

On **i**-PDMS, the adhesive force regime during approach was deeper than on **i**-LBL, about 1 μm (Fig. 4C), but capillary bridges with a similar range of adhesive force (10 to 15 μN) and length (13 μm) were observed upon retraction, as expected, because we used the same lubricant for both samples. The noninfused PDMS and commercial foul-release coatings showed a larger adhesive force upon contact (35 μN) but a much smaller displacement length of 1 μm (fig. S10), which we attribute to the Johnson, Kendall, Roberts soft adhesive contact (*38*, *39*). We schematically summarize the force-displacement response for lubricant-infused surfaces in Fig. 4, D and E, and assume the following time-dependent force profile experienced by a mussel foot probing the surface (Fig. 4F): Before any contact, the mussel foot senses an (unexpected) adhesive capillary force; provided the mussel keeps probing, its foot will eventually detect the larger moduli of the solid surface below the lubricant layer, whereas it will again

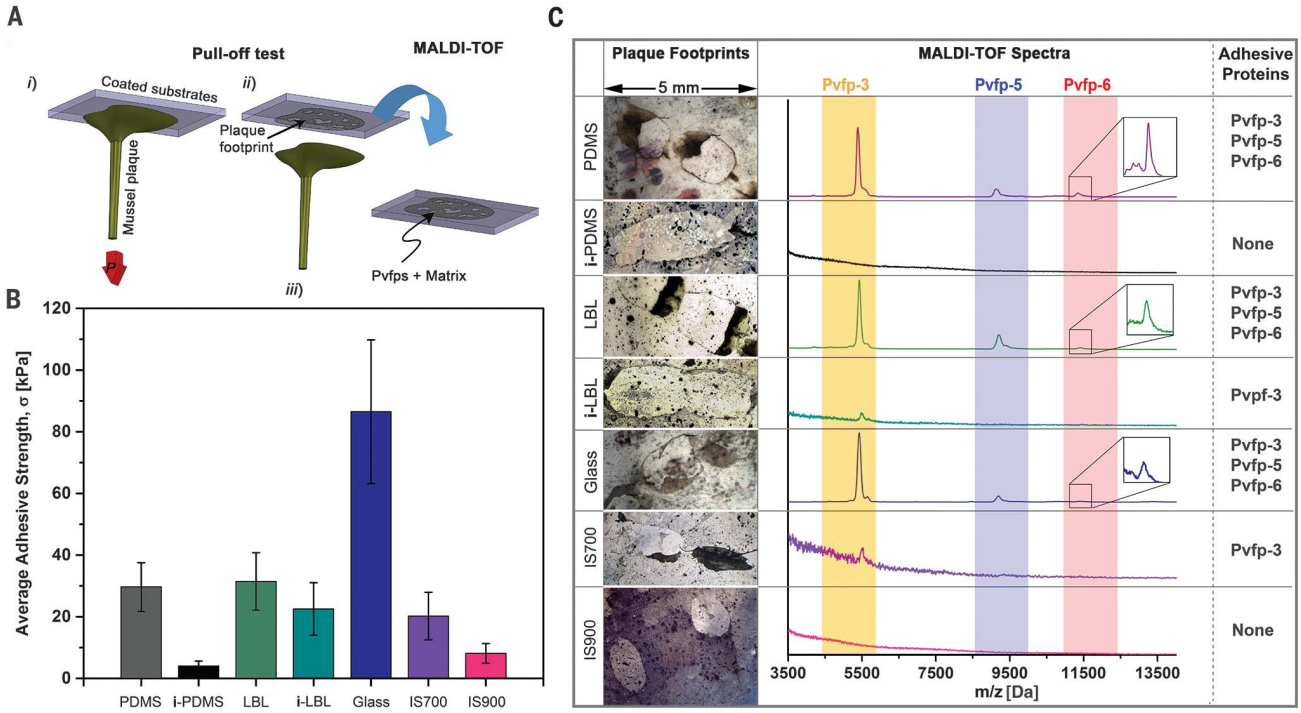

Fig. 2. Analysis of *P. viridis* adhesive footprint by MALDI-TOF and adhesive strength. (**A**) Schematic representation of the experiments. (**B**) Average adhesive strength on different surfaces. All measurements for **i**-PDMS were obtained from the only 1 of 15 **i**-PDMS samples onto which plaques were deposited. Values are mean ± SD. (**C**) MALDI-TOF spectra of mussel plaque footprints after plaque detachment. The absence or low signal intensity of adhesive proteins (Pvfps) indicate weak nonspecific adsorption and, consequently, effective antifouling activity.

Fig. 3. Antifouling performance of i-PDMS, PDMS, and IS900 panels in the field. (**A**) Representative images for the fouling communities associated with each surface type after 8 and 16 weeks of static immersion on 175 mm by 175 mm substrates at Scituate Harbor, MA, USA. Slime: microalgal films; Soft: tunicates, hydroids, and macroalgae; Hard: mussels. (**B**) Total coverage and composition of the fouling communities.

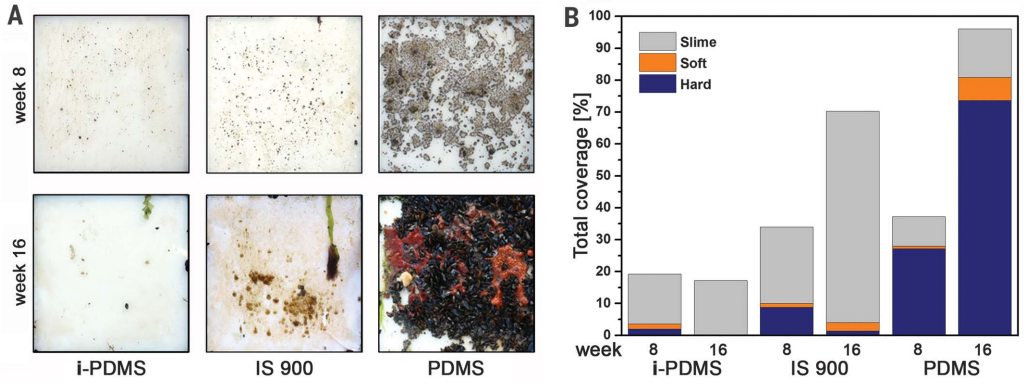

experience adhesive capillary forces upon partial retraction.

On the mechanism of mussel attachment to lubricant-infused surfaces

For efficient fouling prevention, a material needs to deter initial attachment and minimize the adhesion strength when a fouler encounters the surface (*7*). Lubricant-infused coatings satisfy and improve upon both criteria. Their solid/liquid composite nature at the nanoscale has key implications for mussel adhesion, because the adhesive plaque is delivered as a viscous secretion (*15*) that will not fully displace the lubricant as long as the lubricant layer remains stable, causing the abnormal plaque secretion (table S1). With transcriptomic analysis (*40*), we confirmed the presence of transient receptor potential (TRP) channels in *P. viridis* feet (table S3), which are implicated in mechanosensing in diverse organs and species (*41*), indicating that tactile sensors may contribute to the sensing mechanism of mussels. We suggest that these channels remain unactivated on infused surfaces, because our nanoscale contact mechanics data indeed imply that the feet would not feel a substantial compressive force after initial contact. In contrast, a tensile force arises due to capillary bridges (Fig. 4, B and C) that may prevent the activation of the TRP channels. We therefore propose that infused surfaces "confuse" the mussels, which frequently appear unable to detect the lubricant-protected solid substrate, and consequently do not deposit plaques (Fig. 1 and table S1). Although **i**-LBL performs better than noninfused controls and is on par with state-of-the-art commercial coatings, a significantly larger number of plaques were deposited on **i**-LBL compared with **i**-PDMS (Fig. 1). Because **i**-LBL exhibits a thinner lubricant layer and is much stiffer than PDMS, we suggest that mussels' probing feet are statistically more likely to reach the underlying surface and experience a relatively higher contact force if they do, thus promoting plaque secretion.

For the few deposited plaques, **i**-PDMS also outperformed all other tested surfaces in terms of adhesive strength (Fig. 2B). Adhesion of fouling organisms has been reasonably well described using linear elastic fracture mechanics (*31*, *32*), which, in the simplest case, predicts the macroscopic adhesion strength to scale as $(E{\cdot}\gamma_s)^{1/2}$. However, this scaling law does not capture the effect of the lubricant. Because E is only slightly affected upon infusion, the 10-fold decrease of σ_{ad} for **i**-PDMS compared with PDMS would imply γ_s of the infused surface to be smaller by a factor of roughly 100, which is not realistic [the surface energy of PDMS and the surface tension of silicone oil, covering the surface in the infused coating, are comparable (SM, section IIC)]. Mussel adhesion is mechanically more complex because the adhesive plaque-thread assembly leads to the coupling between the local work of adhesion w_a (molecular-level interfacial energy) and the elastic strain energy W_e stored in the plaque-thread structure (Fig. 5). In analogy to the valve concept in fracture mechanics (*42*, *43*), developed to describe interfacial fracture phenomena in the presence of dissipative mechanisms away from the fractured surfaces, the total adhesion energy during decohesion G_c can be described as the sum of both contributions.

$$G_c = w_a + W_e \quad (1)$$

Pull-off energies of individual threads are on the order of 1 J/m^2 (*35*, *36*), whereas w_a measured for individual adhesive proteins range from 0.1 to 0.01 J/m^2 (*44*, *45*), illustrating that W_e is orders of magnitude higher than w_a (*35*). According to the valve concept, even though W_e is far greater than w_a in the presence of dissipative processes, w_a still governs fracture because W_e directly depends on w_a that acts as an amplifying "valve" for dissipative mechanisms (*46*, *47*). For viscoelastic adhesion, which is relevant for mussel adhesion, G_c is proportional to w_a (*48*)

$$G_c = w_a{\cdot}\phi(da/dt, T, \varepsilon) \quad (2)$$

where ϕ is a mechanical dissipative function that depends on the crack growth rate da/dt, the temperature T, and the macroscopic strain ε. The key implication is that even a small reduction

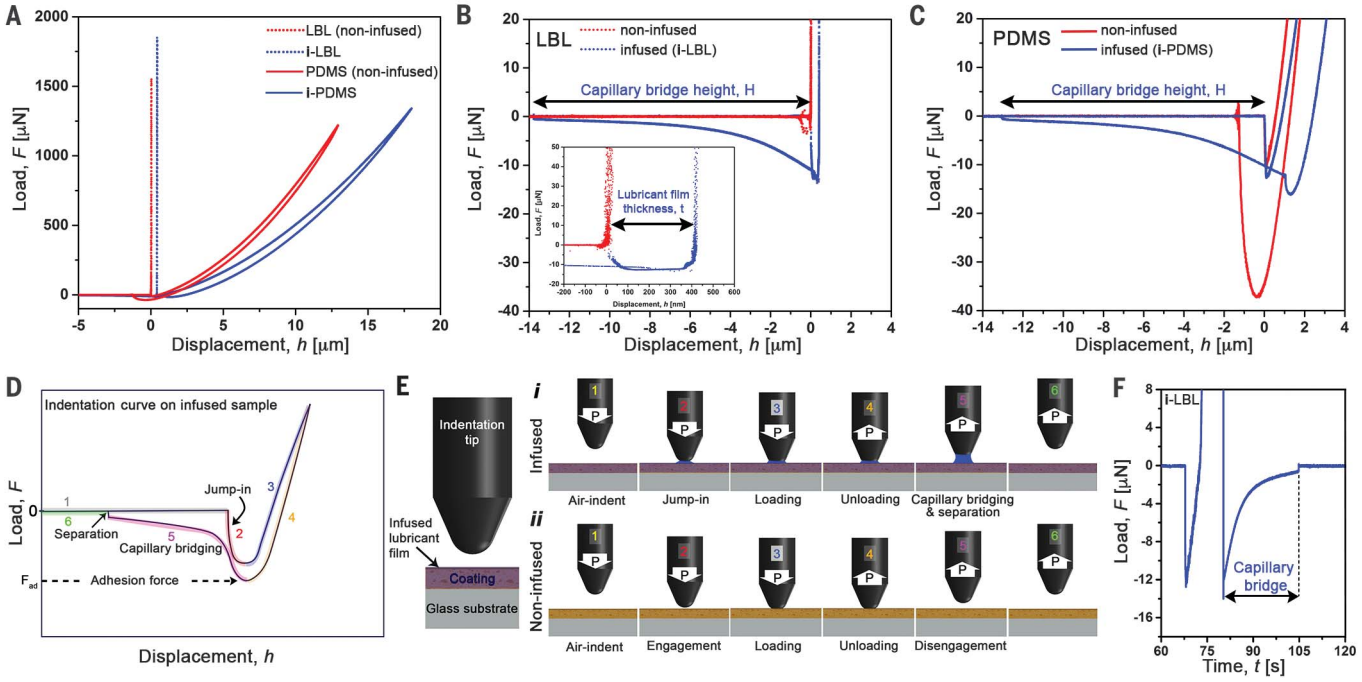

Fig. 4. Nanoscale contact mechanics of LBL, PDMS, i-LBL, and i-PDMS surfaces. (**A**) Characteristic load-displacement curves obtained using a conospherical tip. (**B** and **C**) Enlargement of the adhesive force regimes for LBL and **i**-LBL (B), and for PDMS and **i**-PDMS (C). Jump-in and jump-off instabilities upon approach and retraction are attributed to capillary bridges of the lubricant. Inset in (B) is an enlargement of the low-displacement region, showing that the lubricant thickness for LBL is about 400 nm. (**D** and **E**) Representative indentation curves of lubricant-infused surfaces (D) and corresponding contact regimes (E). Upon approach ("1"), a capillary bridge is formed with equal adhesive force on both soft PDMS and stiff LBL surfaces ("2"), followed by forces arising from the solid material ("3" and "4"). During retraction, an adhesive force retains due to the formation of a capillary bridge ("5"), the length of which is roughly equivalent between the two types of surfaces, indicating that the effect is entirely mediated by the lubricant. (**F**) Force profile over time during contact on an infused surface, mimicking the force profile "sensed" by mussel feet during surface exploration.

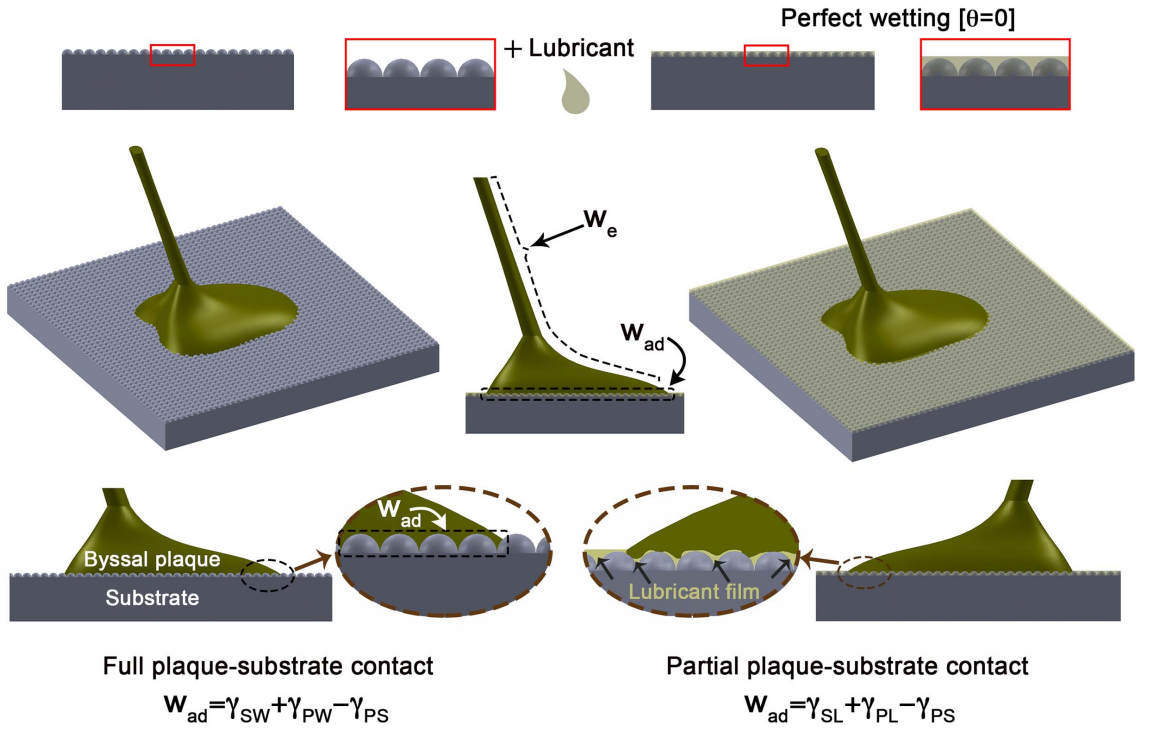

Fig. 5. Adhesion mechanics of mussel threads on noninfused (left) and infused (right) surfaces. The total adhesion energy G_c is the sum of the thermodynamic work of adhesion w_a at the interface (molecular interfacial energy due to the adhesive proteins) and of the viscoelastic dissipative process due to plaque and thread deformation (W_e). For the noninfused surface, the liquid is water, whereas for the infused surfaces, the liquid is the infused lubricant. The vanguard Pvfp-5 adhesive protein efficiently displaces molecular-bound water on noninfused surfaces (*15*), whereas residual lubricant may remain at the interface for the infused surfaces, owing to the ultralow interfacial energy between the substrate and the lubricant, leading to partial plaque/substrate contact.

in w_a leads to a large decay in G_c, and thus to an enhanced foul-release efficiency. w_a for the infused sample is predicted to be appreciably smaller because of the low interfacial energy of the lubricant/substrate interface (SM, section IIC). From calculations, we find a lower interfacial energy for **i**-PDMS compared with **i**-LBL (SM, section IIC) (fig. S11), which is in qualitative agreement with the better macroscopic antifouling performance of **i**-PDMS.

In addition, the effective plaque/substrate contact area may be decreased because the entrapped lubricant is not fully displaced by Pvfp-5 (Fig. 5, lower right), as supported by the absence of Pvfp-5 on **i**-PDMS (Fig. 2C). These two effects synergistically combine to decrease w_a for the infused surfaces, thus minimizing amplification and preventing the activation of larger-scale dissipative mechanisms in the plaque/thread assembly away from the interface.

Conclusion

Lubricant-infused surfaces exhibit remarkable, biocide-free nonfouling activity—both in the laboratory and in the field—against mussels, one of the most pervasive marine macrofoulers. Our comprehensive study across multiple length scales suggests fundamental mechanisms behind this antifouling performance. First, lubricant-infused surfaces deter the attachment because the lubricant overlayer may deceive the mechanosensing mechanism of mussels that trigger their adhesive behavior only upon detecting the solid surface. Second, the resulting low attachment frequency is accompanied by much lower attachment strength. The entrapped lubricant affects the molecular work of adhesion, which, by virtue of the valve effect, substantially decreases macroscopic adhesion. Both types of infused surfaces reduce attachment, with **i**-PDMS showing the strongest antifouling behavior. Importantly, the latter can be formulated into a sprayable paint, allowing for an easy, large-scale application on arbitrary surfaces and for long-lasting performance due to diffusion and effective replenishment of the lubricant through the polymeric coating (*27*). Our findings show that lubricant-infused materials are promising to address the important economic and ecological burdens associated with marine biofouling, especially those triggered by the invasion of mussel species.

REFERENCES AND NOTES

1. A. I. Railkin, *Marine Biofouling: Colonization Processes ad Defenses* (CRC Press, Boca Raton, FL, USA, 2004).
2. H.-C. Flemming, P. Sriyutha Murthy, R. Venkatesan, K. E. Cooksey, Eds., *Marine and Industrial Biofouling* (Springer-Verlag, Berlin, Germany, 2009).
3. L. D. Chambers, K. R. Stokes, F. C. Walsh, R. J. K. Wood, *Surf. Coat. Tech.* **201**, 3642–3652 (2006).
4. M. Salta *et al.*, *Philos. Trans. R. Soc. A* **368**, 4729–4754 (2010).
5. M. P. Schultz, J. A. Bendick, E. R. Holm, W. M. Hertel, *Biofouling* **27**, 87–98 (2011).
6. I. Banerjee, R. C. Pangule, R. S. Kane, *Adv. Mater.* **23**, 690–718 (2011).
7. M. Lejars, A. Margaillan, C. Bressy, *Chem. Rev.* **112**, 4347–4390 (2012).
8. S. Dürr, J. C. Thomason, *Biofouling* (Blackwell Publishing Ltd., Oxford, UK, ed. 1st, 2010).
9. B. P. Lee, P. B. Messersmith, J. N. Israelachvili, J. H. Waite, *Annu. Rev. Mater. Res.* **41**, 99–132 (2011).
10. J. H. Waite, *Nat. Mater.* **7**, 8–9 (2008).
11. J. H. Waite, M. L. Tanzer, *Science* **212**, 1038–1040 (1981).
12. J. Yu *et al.*, *Proc. Natl. Acad. Sci. U.S.A.* **110**, 15680–15685 (2013).
13. W. Wei, J. Yu, C. Broomell, J. N. Israelachvili, J. H. Waite, *J. Am. Chem. Soc.* **135**, 377–383 (2013).
14. G. P. Maier, M. V. Rapp, J. H. Waite, J. N. Israelachvili, A. Butler, *Science* **349**, 628–632 (2015).
15. L. Petrone *et al.*, *Nat. Commun.* **6**, 8737 (2015).
16. W. Wei *et al.*, *Acta Biomater.* **10**, 1663–1670 (2014).
17. T.-S. Wong *et al.*, *Nature* **477**, 443–447 (2011).
18. A. K. Epstein, T. S. Wong, R. A. Belisle, E. M. Boggs, J. Aizenberg, *Proc. Natl. Acad. Sci. U.S.A.* **109**, 13182–13187 (2012).
19. J. Li *et al.*, *ACS Appl. Mater. Interfaces* **5**, 6704–6711 (2013).
20. N. MacCallum *et al.*, *ACS Biomater. Sci. Eng.* **1**, 43–51 (2015).
21. U. Manna *et al.*, *Adv. Funct. Mater.* **26**, 3599–3611 (2016).
22. J. Bruchmann, I. Pini, T. S. Gill, T. Schwartz, P. A. Levkin, *Adv. Healthc. Mater.* **6**, 1601082 (2017).
23. S. Wang, K. Liu, X. Yao, L. Jiang, *Chem. Rev.* **115**, 8230–8293 (2015).
24. F. Schellenberger *et al.*, *Soft Matter* **11**, 7617–7626 (2015).
25. J. D. Smith *et al.*, *Soft Matter* **9**, 1772–1780 (2013).
26. S. Sunny, N. Vogel, C. Howell, T. L. Vu, J. Aizenberg, *Adv. Funct. Mater.* **24**, 6658–6667 (2014).
27. J. Cui, D. Daniel, A. Grinthal, K. Lin, J. Aizenberg, *Nat. Mater.* **14**, 790–795 (2015).
28. S. Sunny *et al.*, *Proc. Natl. Acad. Sci. U.S.A.* **113**, 11676–11681 (2016).
29. L. Xiao *et al.*, *ACS Appl. Mater. Interfaces* **5**, 10074–10080 (2013).
30. A. B. Tesler *et al.*, *Nat. Commun.* **6**, 8649 (2015).
31. R. F. BradyJr., I. L. Singer, *Biofouling* **15**, 73–81 (2000).
32. J. Y. Chung, M. K. Chaudhury, *J. Adhes.* **81**, 1119–1145 (2005).
33. J. W. Chapman, T. W. Miller, E. V. Coan, *Conserv. Biol.* **17**, 1386–1395 (2003).
34. J. R. Burkett, J. L. Wotjas, J. L. Cloud, J. J. Wilker, *J. Adhes.* **85**, 601–615 (2009).
35. K. W. Desmond, N. A. Zacchia, J. H. Waite, M. T. Valentine, *Soft Matter* **11**, 6832–6839 (2015).
36. Z. Qin, M. J. Buehler, *Nat. Commun.* **4**, 2187 (2013).
37. N. R. Martinez Rodriguez, S. Das, Y. Kaufman, J. N. Israelachvili, J. H. Waite, *Biofouling* **31**, 221–227 (2015).
38. J. N. Israelachvili, *Intermolecular and Surface Forces* (Academic Press, ed. 3, 2011).
39. M. K. Chaudhury, *J. Adhes. Sci. Technol.* **7**, 669–675 (1993).
40. P. A. Guerette *et al.*, *Nat. Biotechnol.* **31**, 908–915 (2013).
41. A. P. Christensen, D. P. Corey, *Nat. Rev. Neurosci.* **8**, 510–521 (2007).
42. J. R. Rice, J. S. Wang, *Mater. Sci. Eng. A* **107**, 23–40 (1989).

43. Z. Suo, C. F. Shih, A. G. Varias, . *Acta Mater.* **41**, 1551–1557 (1993).
44. D. S. Hwang *et al*., *J. Biol. Chem.* **285**, 25850–25858 (2010).
45. E. W. Danner, Y. Kan, M. U. Hammer, J. N. Israelachvili, J. H. Waite, *Biochemistry* **51**, 6511–6518 (2012).
46. D. M. Lipkin, G. E. Beltz, *Acta Mater.* **44**, 1287–1291 (1996).
47. A. Miserez, A. Rossoll, A. Mortensen, *Acta Mater.* **52**, 1337–1351 (2004).
48. A. J. Kinloch, *Adhesion and Adhesives Science and Technology* (Springer-Science Business Media, 1987).

ACKNOWLEDGMENTS

This study was funded by the Singapore Maritime Institute (SMI), grant SMI-2013-MA-03 (A.M.). This work was also funded by the Advanced Research Projects Agency-Energy (ARPA-E), U.S. Department of Energy, under award DE-AR0000326, and by the Office of Naval Research (ONR), U.S. Department of Defense, under award N00014-16-1-3169. N.V. acknowledges funding of the Deutsche Forschungsgemeinschaft (DFG) through the Cluster of Excellence Engineering of Advanced Materials (EXC 315) and the Interdisciplinary Center for Functional Particle Systems (FPS). We thank A. Tesler for providing **i**-WO samples, D. Daniel for discussion on interfacial energies, E. Maldonado for help with the field study, and Stellwagen Bank National Marine Sanctuary for providing the field site and field site support. The transcriptome of *P. viridis* foot used to identify TRP channels is available at https://www.ncbi.nlm.nih.gov/nuccore/GEKL00000000. S.S., N.V., and J.A. are inventors on a patent application (US20150210951A1) submitted by Harvard University that covers LBL slippery liquid-infused porous surfaces (SLIPS). J.A. is an inventor on a U.S. Patent Application (# 14/414,291) submitted by Harvard University that covers 3D SLIPS. J.A. is the founder of the start-up company SLIPS Technologies, Inc.

SUPPLEMENTARY MATERIALS

www.sciencemag.org/content/357/6352/668/suppl/DC1
Materials and Methods
Supplementary Text
Figs. S1 to S11
Tables S1 to S3
Movies S1 to S7
References (*49*–*66*)

27 August 2016; resubmitted 20 February 2017
Accepted 20 July 2017
10.1126/science.aai8977

Preventing mussel adhesion using lubricant-infused materials

Shahrouz Amini, Stefan Kolle, Luigi Petrone, Onyemaechi Ahanotu, Steffi Sunny, Clarinda N. Sutanto, Shawn Hoon, Lucas Cohen, James C. Weaver, Joanna Aizenberg, Nicolas Vogel and Ali Miserez

Science **357** (6352), 668-673.
DOI: 10.1126/science.aai8977

When you don't want things to stick

During marine fouling, surfaces are encrusted with scale or biological organisms, which can be expensive to remove. Amini *et al.* used polymers infused with organic lubricants to prevent mussels from adhering to a submerged surface. The infused polymer presents a relatively soft surface to the mussel. This means that when the mussel probes the surface with its feet, it is less likely to release adhesive threads, which reduces its adhesion. The antifouling properties of the treatment were observed in both a laboratory setting and field testing.

Science, this issue p. 668